Influence of Land Surface Temperature and Rainfall on Surface Water Change: An Innovative Machine Learning Approach

Influence of Land Surface Temperature and Rainfall on Surface Water Change: An Innovative Machine Learning Approach

Vanita Jain[1] · Aarushi Dhingra[1] · Eeshita Gupta[1] · Ish Takkar[1] · Rachna Jain[2] · Sardar M. N. Islam[3]

Abstract
The largest reservoir of drinkable water on Earth is surface water. It is crucial for maintaining ecosystems and enabling people to adapt to diverse climate changes. Despite surface freshwater is essential for life, the current research shows a striking lack of understanding in its spatial and temporal dynamics of variations in outflow and storage across a sizable country: India. Numerous restrictions apply to current research, including the use of insufficient machine learning techniques and limited data series. This work uses cutting-edge and SOTA-method to use the available data and machine learning to accurately understand spatial and temporal dynamics of variations in surface freshwater outflow and storage using extended data series. The authors did the examination of thematic maps produced using ArcMap 10.8 from June'2005 to June'2020 using JRC dataset to track changes in the intensity of surface water. Google Earth Engine in Python API has been devised to detect changes in surface water levels and quantifying shifting map trends. Raster image viewing, editing, and calculation are done with ArcMap. For determining the relationship between declines in Surface water levels, changes in rainfall intensity and land surface temperature, variables were averaged over 13 rivers for 15 years. The change in surface water is reliant on independent variables of change in land surface temperature and rainfall intensity. The authors use the correlation between these parameters to achieve an average R-squared adjusted value of 0.402. The study's findings contribute to a better understanding of the matter and can be used across the world.

1 Introduction

Surface water comprises less than one-thousandth of a percent of the total water on the planet but is still an essential resource because it helps serve many critical functions of human life and the environment (Prigent et al. 2007; Downing et al. 2006). Surface Water

✉ Sardar M. N. Islam
  sardar.islam@vu.edu.au

Extended author information available on the last page of the article

is the primary drinking water resource and for many other daily activities. Over the past few years, a decline in surface water intensity has been reported in India, making monitoring surface freshwaters a high-priority task for the betterment of water management and climate research (Vorosmarty et al. 2000; Shindell et al. 2005). An effective method for studying the quantitative and qualitative changes occurring on surface water bodies can be established by utilizing appropriate digital image processing techniques on images taken from remote sensing satellites or aerial sensors. Multispectral and hyperspectral images captured by various remote sensing satellites provide abundant information. The potential of remote sensing technologies for analyzing natural resources like water has been extensively researched over the past years. This research uses remote sensing technologies to analyze the difference in the surface water levels using the JRC Dataset obtained using Landsat Satellite images. Furthermore, his study focuses on 2 major factors to derive the relationship for the surface level changes: (1) Land Surface Temperature and (2) Rainfall Intensity. After analyzing all three factors, the study concludes that the Land Surface Temperature drastically impacts surface water levels. The places where the increase in land surface temperature are high show a drastic decrease in the surface water level, indicating that global warming plays an important role in the decline. The worst impacted places showed the maximum increase in the land surface temperature and a sharp decline in rainfall levels. Surface water levels have shown positive changes for places where the temperature remained constant, which could lead the author to a probable solution to the problemat hand. Surface water levels improve if steps are taken to normalize the high temperatures due to Global Warming. This can be done by minimizing carbon footprint, decline in the use of greenhouse gases, reducing industrialization, population control, and afforestation. Rainwater harvesting and proper irrigation practices for storing and utilizing rainwater efficiently are some ways that can help maintain surface water levels.

2 Related Work, Limitations, Objectives and Contributions

Surface water presence varies widely and is necessary for the survival of living beings. It is an ideal predictor of the change of the environment. Precise and up-to-date knowledge on the spatial water flow is a cornerstone for various science activities such as mapping surface water inventories, measuring water for drinking purposes and drainage, mapping and modifying land use/landscape. Remote sensing is a fast-expanding technique that provides accurate, low-cost, reliable, and even real-time data gathered for local, regional, and global environmental change. High-resolution mapping and long-term variations of worldwide surface water are provided by Jean-Francis Pekelet al. (2016). The paper describes in detail the data sets available as part of the global Surface Water Dataset of the Joint Research Centre. It gives an objective, description, and symbology for each dataset for users to comprehend and utilize each dataset effectively and properly.

The idea of temporal stability analysis (TSA) was used by Zhang et al. (2022) to investigate the temporal aspects of spatial variability in surface water quality in the Chinese river Qiantang. In contrast to mean absolute bias error (MABE) and root mean square, their research indicated that standard deviation of the relative difference (SDRD) and the index of temporal stability (ITS) were more effective at finding stable sites (RMSE).

Singh and Dhadse (2021) used the Ganges River as a case study and created a framework for a climate change policy. They developed the Climatic Sustainability Index (CSI), which assisted in assessing the economic viability of a geographical area vulnerable to climatic change.

In Rajshahi City Corporation (RCC) districts, Al Kafy et al. (2021) initially z recognized the changes in land usage and land consumption (LULC) pattern and looked into their effects on land surface temperature (LST They forecasted the seasonal LST situations for 2030 and 2040 using an ANN algorithm in the MATLAB software. This study offered a practical plan for guaranteeing sustainable land use management, temperature reduction, and potential mitigating actions to counteract the effects of climate change.

Using multi-temporal satellite imagery, Puppala and Singh (2021) examined the urban heat island effect (UHI) in Vishakhapatnam, India. They found that a rise in UHI has a detrimental effect on LST and LULC.

In the north-western region of Iran, on the Hashtgerd Plain, Mehrazaret al. (2020) investigated the effects of climate change on agricultural, water resource, and socioeconomic activities. To investigate the effects of climate change on various subsystems, they developed a system dynamics model. Their model was able to depict the dynamic interactions between the changing climate and numerous subsystems at the watershed level.

Barakat et al. (2019) evaluated the environmental effect of the remote sensing, geographical information system (GIS) and fuzzy analytical hierarchy process (FAHP) in the cities in Béni-Mellal, and the neighbouring communities (Morocco) between 2002 and 2016. The usual LULCC dynamics were measured with remote sensing of the picture linked with the GIS. According to Alsdorf et al. (2007), measurements of the inundated area have been used as proxies for discharge with varying degrees of accuracy, but they are successful only when in situ data is available for calibration; they fail to indicate the dynamic topography of water surfaces, which explains a future satellite concept, the Water and Terrestrial Elevation.

With the growth of artificial intelligence and comprehensive data, feature extraction has become a common research subject in recent years. For example, in Landsat scenes with a mixed water pixel on small rivers or shallow water in China, Jiang et al. (2014) suggested an automatic method for the retrieval of rivers and lakes by integrating water indices (NDWI, mNDWI, AWEIsh and AWE Insh) with digital imaging techniques. Jiang et al. More information on surface water identification, extraction, and tracking with optical remote sensing can be found in the latest study of Huang et al. (2018). Shakeel et al. (2019) took on the complex situation of counting built structures in satellite images. The built-up area segmentation is a more accurate measure of population density, urban area development, and its influence on the environment than building density. They presented a deep learning-based regression approach for counting built structures in satellite images.

Xia and Zeng (2022) used two common types of machine learning techniques, Support Vector Machine (SVM) and Artificial Neural Networks (ANN), to compare and achieve the prediction of the entropy water quality index (EWQI).. Entropy was used in their study to build the network structure of the information set because it is known that the more entropy there is, the more certain an event is to occur. They came to the conclusion that the SVM model in combination with DE-GWO optimization had a great deal of potential for achieving the prediction of EWQI and water quality grade.

To predict rainfall, Pérez-Alarcón et al. (2022) created a hybrid model using ARIMA and artificial neural networks (ANN). Their research can be used to develop trustworthy methods for forecasting rainfall time series for water management.

Mustafa et al. (2020) compared four soft computing techniques, including multivariate adaptive regression splines (MARS), wavelet neural network (WNN), adaptive neuro-fuzzy inference system (ANFIS), and dynamic evolving neural fuzzy inference system (DENFIS), to find the best model for predicting LST changes in Beijing. Topography change was taken into account in the study to correctly forecast LST, and Landsat 4/5 TM and Landsat 8OLI TIRS pictures were utilized to zanalyze LST variations in the research region for four years (1995, 2004, 2010, and 2015). The effects of numerous variables on delta flood were measured by Tang et al. (2016). To measure the influence of these driving variables in the PRD, a technique was devised that included a numerical model and the index R (Tang et al. 2016).

Zha et al. (2003) proposed an unprecedented method for the automation of the process of mapping built-up areas based on the Normalized Difference Built-Up Index. Built-up areas are effectively mapped through arithmetic manipulation of re-coded Normalized Difference Vegetation Index (NDVI) and NDBI images derived from TM imagery. The NDBI method was applied to map urban land in the city of Nanjing, eastern China.

Ghorbani et al. (2022) created a stepwise M5 tree model method to identify the variables that have an impact on rainfall forecast and fixed the algorithm's greedy issue. They also came to the conclusion that the delayed effects of teleconnections can be viewed as a useful characteristic for early rainfall prediction and interannual variation capture. Both continuous (regression) and discrete (classification) data can be used with their method.

Taylor et al. (2013) devised a remote sensing method based on multi-satellite data that offers a global estimate of land-surface open water's monthly distribution and size. The results show significant seasonal and inter-annual variability in inundation extent, with a worldwide average maximum flooded area reduction of 6% throughout the fifteen years, particularly in tropical and subtropical South America and South Asia.

Prigent et al. (2012) developed a novel remote sensing approach to estimate the effect of change in population density from 1973 to 2007 on the surface water levels of tropical and subtropical South America and South Asia and saw an inverse relationship between the two factors.

Wolfe (2006) enumerates the expansion of Satellite Remote Sensing for Earth Science in the Earth Science Remote Sensing monograph. It also discusses the NPOESS and NPP missions. It gives emphasis on MODIS on board both Terra and Aqua. This monograph has been designed to give scientists and research students with limited remote sensing backgrounds a thorough introduction to current and future NASA, NOAA and other Earth science remote sensing missions.

2.1 Limitations of the Existing Literature

There are several limitations of the existing literature in the area of this study: First, in the existing studies, the data series are not sufficiently long, and the consequent modelling and forecasting exercises may not be fully reliable for this reason. Remote Sensing data is essential to monitor the global surface water levels, especially now when the in situ data is rapidly declining. The satellite data, along with the information on the time of capture, makes it possible to analyze the change in surface water levels over the years, but the availability of adequate long-term data still limits researchers. Hydrologic processes are characterized by the frequency with which events of a given magnitude and duration occur. Infrequent but large-magnitude events (floods, droughts) have very large economic, social, and ecological impacts. Without an adequately long record of monitoring data, it is difficult, if not impossible, to understand, model, and predict such events and their effects. Second, another limitation is the

inaccuracy of the mapped data performed using deep learning techniques. Surface water mapping using various methods like deep learning has taken place in various previous researches, but many of them show a lot of false positives. These false positives arise mainly from the ice and snow, which is mistaken to be water bodies due to terrain or cloud shadows.

2.2 Objectives and Contributions of this Paper

The objective of the study is to analyze the changes in the surface water levels of India and to integrate the results with the temperature changes in that area along with the rainfall intensity change from the year 2005–2020. The changes will be mapped using ArcMap, and data analysis will be performed.

The structure of the paper is as follows: In Section 3, the Area of Interest is evaluated, and datasets are specified. Section 4 reports how the data obtained were processed, and raster maps were generated for further investigation of the relationships. Later on, pixel values of specific water bodies were averaged, and the results are reported in Section 5. The paper is finally concluded in Section 6.

3 Specifications

3.1 Study Area

The study area of this work is the Republic of India, a South Asian country extending from latitudes 8°4'N and 37°6'N and longitudes 68°7'E and 97°25'E. It is the second-most populous nation, the seventh biggest by region. The Arabian Sea borders India on the southwest, the Bay of Bengal on the southeast, and the Indian Ocean in the south. India is a water rich country that comprises roughly 4% of the world's water resources (India-WRIS wiki 2015). Rivers have played a major role in the preservation and growth of India's culture. There are nearly 400 rivers (12 major rivers contribute the majority of surface water), some canals, other inland water bodies like brackish water, ponds, and lakes which are unevenly distributed in India. Therefore, the monitoring and estimation of surface water is an essential task. Surface water has different characteristics such as varying temperature, turbidity, depth, and vegetation cover, for which remote sensing technology plays a vital role (Table 1).

For the purpose of extraction of the water bodies in India as shown in Fig. 10, the authors have used the shape file of the Indian region as shown in Fig. 1.

Table 1 Description of datasets

| S.No	Name of the dataset	Purpose of the dataset
1	Joint Research Centre's Global Surface Water	Used to capture difference in the surface level occurrence intensity values over the years
2	Moderate Resolution Imaging Spectroradiometer (MODIS) Land-Surface Temperature/Emissivity (LST) Version 6.0	The thermalband of this dataset is used to evaluate the temperature of the land averaged over a month
3	Precipitation Estimation from Remotely Sensed Information using Artificial Neural Networks	Used to measure rainfall intensity
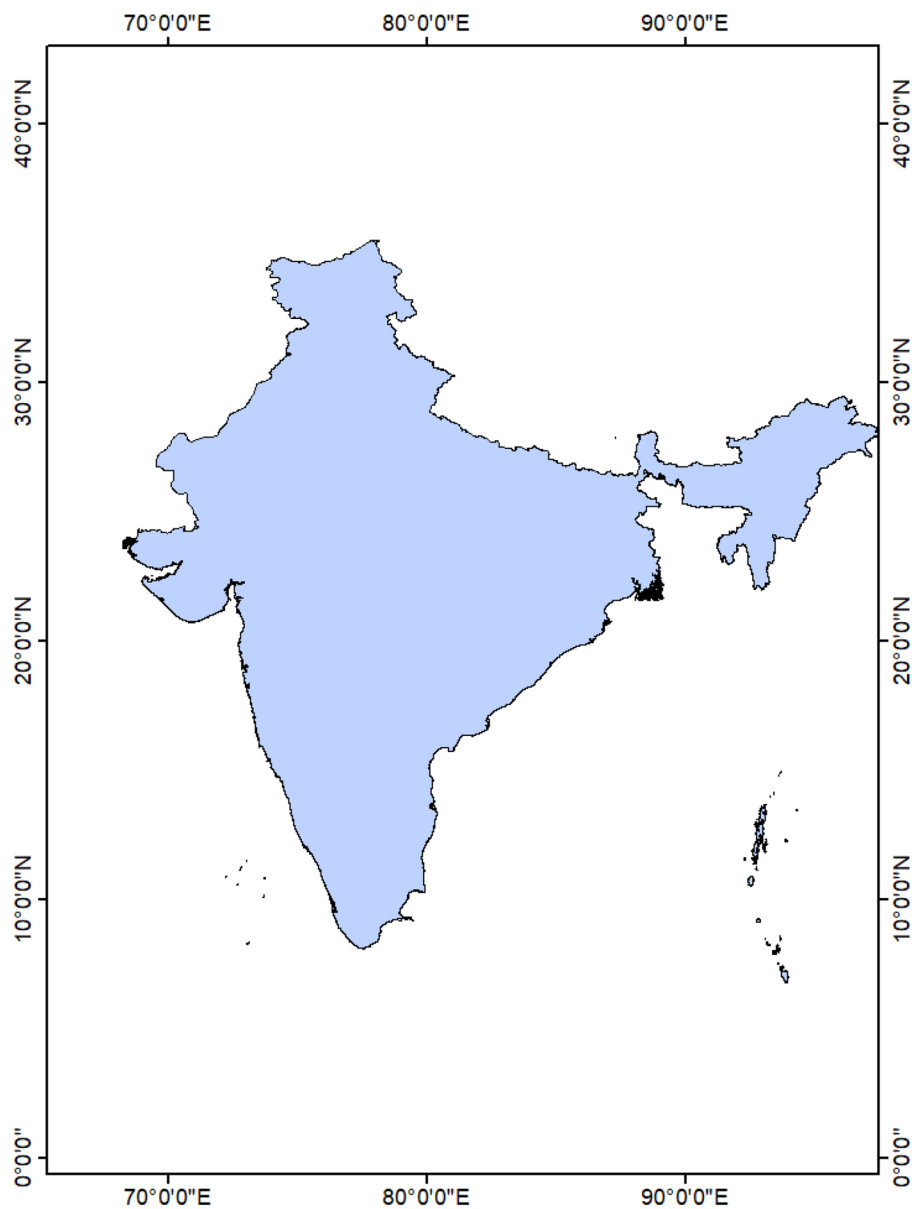
Fig. 1 Shape file of India

3.2 Data

3.2.1 JRC GSW

Joint Research Centre's Global Surface Water (JRC GSW) is a dataset by the European Commission (available from 1984–2020) which attempts to capture the dynamism of

surface water extent at a monthly time scale using high-resolution Landsat data. It was designed using complex decision trees and consists of various global surface water characteristics at 30 m resolution, including occurrence, occurrence change intensity, seasonality, recurrence, transitions, and maximum water extent (JRC Global Surface Water 2000; MODIS Land Surface Temperature 2000; PERSIANN Precipitation Data 2000). The layer used in this study was the Occurrence Change Intensity and was viewed and evaluated using Google Earth Engine in Python API.

The Occurrence Change Intensity map provides information on where the surface water occurrence increased, decreased, or remained the same between 2005–2020. Both the direction of change and its intensity are documented. A difference in water occurrence intensity between two epochs (June 2005 to June 2020) was produced. This is derived from homologous pairs of months (that is, the same months contain valid observations in both epochs). The occurrence difference between epochs was computed for each pair, and differences between all homologous pairs of months were then averaged to create the surface water occurrence change intensity map. Areas, where there are no pairs of homologous months could not be mapped. The averaging of the monthly processing mitigates variations in data distribution over time (that is, both seasonal variation in the distribution of valid observations, temporal depth, and frequency of observations through the archive) and provides a consistent estimation of the water occurrence change. An example of the Occurrence Change Intensity dataset is shown in Fig. 2 for Hooghly River.

Increases in water occurrence are shown in green, and decreases are shown in red. Black areas are those areas where there is no significant change in the water occurrence during the 2005–2020 period. The intensity of the colour represents the degree of change (as a percentage). For example, bright red areas show a greater loss of water than light red areas. Some areas appear grey in the maps; these are locations where there is insufficient data to compute meaningful change statistics. The same is explained in Table 2; the colour code and its significance are provided.
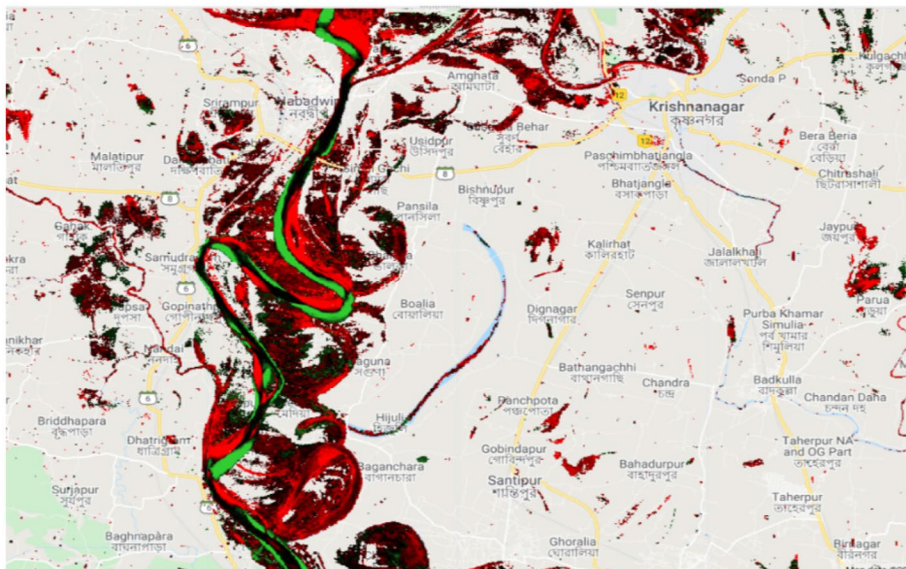
Fig. 2 Changes in occurrence of water from 2005–2020 in Hooghly River, Kolkata, India

Table 2 Colour Palette Symbology

S.No.	TIFF Value	GEE Value	Colour	HEX Value	Significance
1	0	-100		#FF0000	100% Decrease in Surface Water level
2	100	0		#000000	No percentage change
3	200	100		#00FF00	100% Increase in Surface Water Level
4	253	MASKED		#FFFFFF	No water body found
5	254	-128		#888888	Unable to calculate a value due to no homologous months
6	255	127		#CCCCCC	No data available

3.2.2 MODIS LST V6

Land Surface Temperature (LST) is the key factor in detecting the overall climate change over a long time. The evaluation of LST was done using the Moderate Resolution Imaging Spectroradiometer (MODIS) Land-Surface Temperature/Emissivity (LST) dataset (Wan 2008). The LST and Emissivity daily data are retrieved at 1 km pixels by the generalized split-window algorithm and at 6 km grids by the day/night algorithm. In the split-window algorithm, emissivity in bands 31 and 32 is estimated from land cover types. Atmospheric column water vapor and lower boundary air surface temperature are separated into tractable sub-ranges for optimal retrieval (Wolfe 2006).

The MODIS LST Ver. 6 (Wan 2008) products provide pixel-by-pixel temperature in Kelvin. MODIS LST products were downloaded onto the system as HDF (Hierarchical Data Format) files. The HDF Files were accessed using ArcMap for June 2005 and June 2020. Further raster calculations were performed with Raster Calculator the ESRI Spatial Analyst extension under the ArcToolbox. The new raster map was created with a scale factor of 0.02 was multiplied.
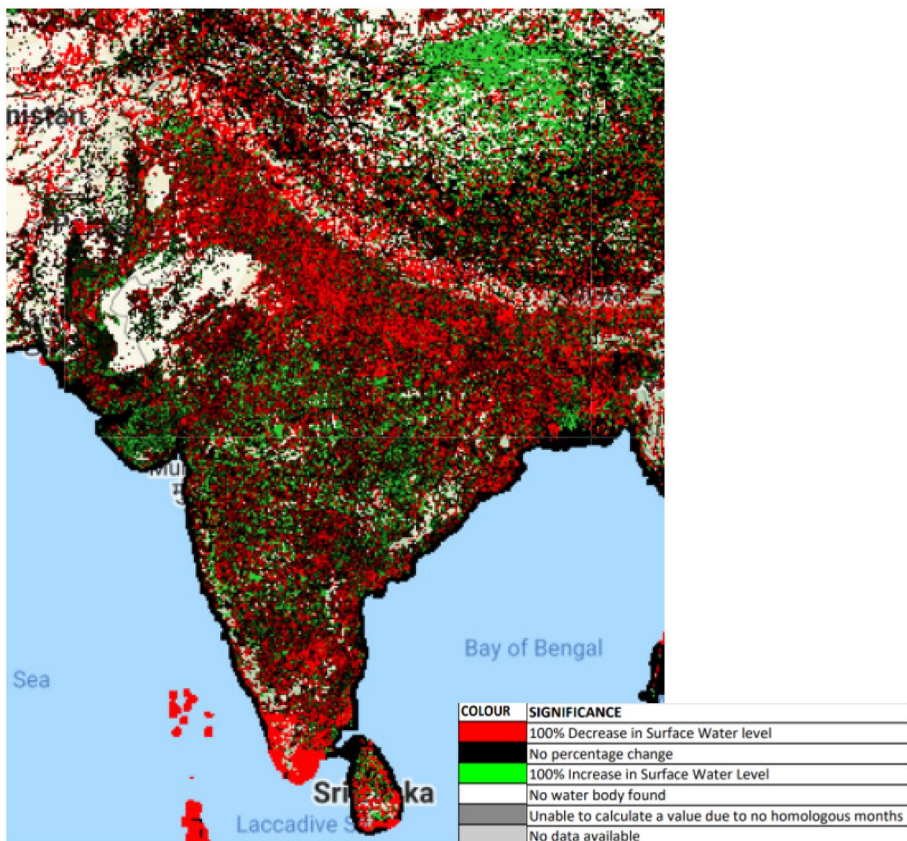
3.2.3 PERSIANN

Rainfall patterns affect human activities and natural resources like groundwater, transient water bodies, and surface water. With the increase in global warming, the rainfall patterns and intensity have been altered and shown huge variation over the last few decades. PERSIANN (Precipitation Estimation from Remotely Sensed Information using Artificial Neural Networks) (PERSIANN 2000) and Nguyen et al. (2019) computes an estimate of rainfall rate at each $0.25° \times 0.25°$ pixel of the infrared brightness temperature image provided by geostationary satellites using neural network function classification/approximation procedures. Whenever independent rainfall estimates are available, an adaptive training feature facilitates an update of the network parameters. The PERSIANN system was based on geo-stationary infrared imagery and later extended to include the use of both infrared and daytime visible imagery. The PERSIANN algorithm used here is based on the geo-stationary longwave infrared imagery to generate global rainfall.

4 Methodology

4.1 Detection of Surface Water Change

Using the JRC dataset, the authors mapped the change in surface water intensity and analyzed the thematic maps (Indian subcontinent) generated using ArcMap 10.8 for June 2005 and June 2020. The Water Occurrence Change Intensity data layer provides a measure of how surface water has changed between two epochs: 2005–2020. The layer averages the change across homologous pairs of months taken from the two epochs. Occurrence change intensity is provided in two ways, both as absolute and normalized values. The absolute values were used, and a raster calculation was performed.

Raster 2 (the year 2020) is subtracted from Raster 1 (year 2005) and the output raster values represent the difference between the two rasters on a pixel-by-pixel basis. Figure 3 indicates occurrences variations over the course of 15 years. The intensity with which incidence grew or decreased demonstrates gains, losses, and consistency in persistence. The red pixels show the decrease in the surface water intensity over the years, whereas the green pixels show the increase in the surface water. The area with no coloured pixels

COLOUR	SIGNIFICANCE
	100% Decrease in Surface Water level
	No percentage change
	100% Increase in Surface Water Level
	No water body found
	Unable to calculate a value due to no homologous months
	No data available

Fig. 3 Change in intensity of surface water of India from 2005 to 2020

is missing data that could not be used for appropriate calculations. The colour palette symbology is explained in Table 2 of Section 3.

This variance might be seen as an impact because of anthropogenic activities, including urban development, forest degradation, and resource exploitation. A rise in surface water was seen in the Himalayan and the peninsula area of India, culminating due to change in land temperature, melting mountain glaciers in the Himalayan region, excessive rainfall in the peninsula and other factors.

4.2 Detection of Changes in Other Factors and Causes

4.2.1 Change in Land Surface Temperature

The rise in greenhouse gases from human activity is largely to blame for rising land surface temperatures. Surface water, glaciers, and ice sheets are all affected by rising land surface temperatures. In the study region, where homogeneous and continuous monitoring is difficult owing to expensive and unreliable equipment and variable seasonality, satellite-derived estimates of land temperature are useful to substitute for observations and data. The Moderate Resolution Imaging Spectroradiometer (MODIS) is a payload imaging sensor built by Santa Barbara Remote Sensing. The instruments capture data in 36 spectral bands ranging in wavelength from 0.4 μm to 14.4 μm and at varying spatial resolutions. The MODIS dataset was used for the research to analyze the Land Surface Temperature Dataset from June 2005 to June 2020.

As measured in the direction of the distant sensor, the radiative skin temperature of the land surface is known as the Land Surface Temperature (LST). It is calculated using Top-of-Atmosphere brightness temperatures from a constellation of geo-stationary satellites' infrared spectral channels. LST is made up of a combination of vegetation and bare soil temperatures because both react quickly to changes in incoming solar radiation caused by cloud cover and aerosol load changes, as well as daily variations in illumination.

The calculation of the change in Land Surface Temperature over the years started by initially downloading the MODIS Dataset LST Band (Mustafa et al. 2020) for both the years June 2005 and June 2020. After obtaining the datasets, ArcMap was used to view the datasets with geospatial references. The datasets were viewed as shown in Fig. 4. After adding both the datasets into the software as 'Layers', ESRI Spatial Analyst extension under the ArcToolbox was used to create a new raster map with the help of the two existing MODIS Datasets. Raster Calculator under 'Map Algebra' was used to create the new map, the flow chart is given in Fig. 4. The output raster was saved in the system and shown in Fig. 5 to carry on the research.

These images were produced using ArcMap10.8; Fig. 5 denotes the land surface temperature of 2005 and Fig. 6 shows the land surface temperature for 2020. Table 3 explains the colour symbology of the thematic maps.

The fluctuation in LST during the 21-year study years is considerable. Some places have had an increase in LST, while others, such as the peninsular plateau, have seen a reduction or no change, as seen in Fig. 6. Pixel by pixel raster calculation was performed on the two maps given above using ArcGIS 10.8 Software on the land surface temperature values of 2005 and 2020. Figure 7 shows the new raster map created where each pixel value is the difference between the LST in 2020 (Raster 2) and 2005 (Raster 1). Using the Formula (1).
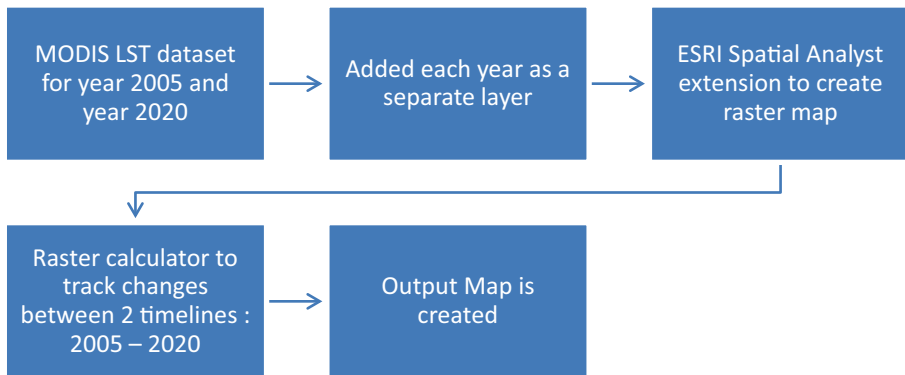
Fig. 4 Flow chart of the Raster Calculation using ArcGis

$$x_{change} = Raster\left(Year\ ''2020''\right) - Raster(Year\ ''2005'')\tag{1}$$

The purple pixels show high positive temperature differences, meaning that the value has increased significantly from 2020 to 2005, whereas the light purple pixels show constant temperatures. On the other hand, the white pixels in Fig. 7 are the negative difference in the temperature levels. This means that the temperature decreased in 2020 as compared to the land surface temperature in the year 2005. Table 4 gives the colour symbology of the map.
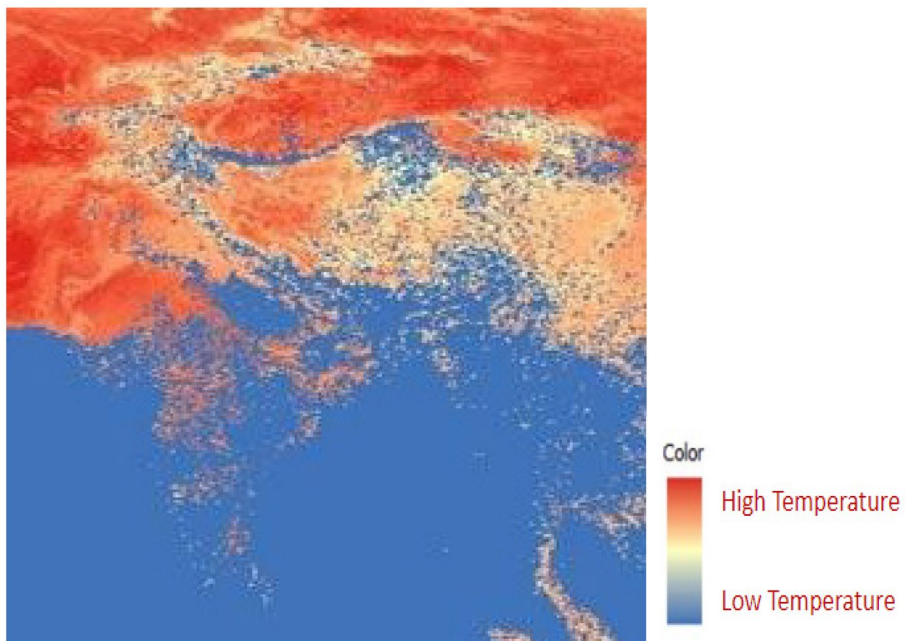
Fig. 5 Land Surface Temperature, Indian Subcontinent, year 2005
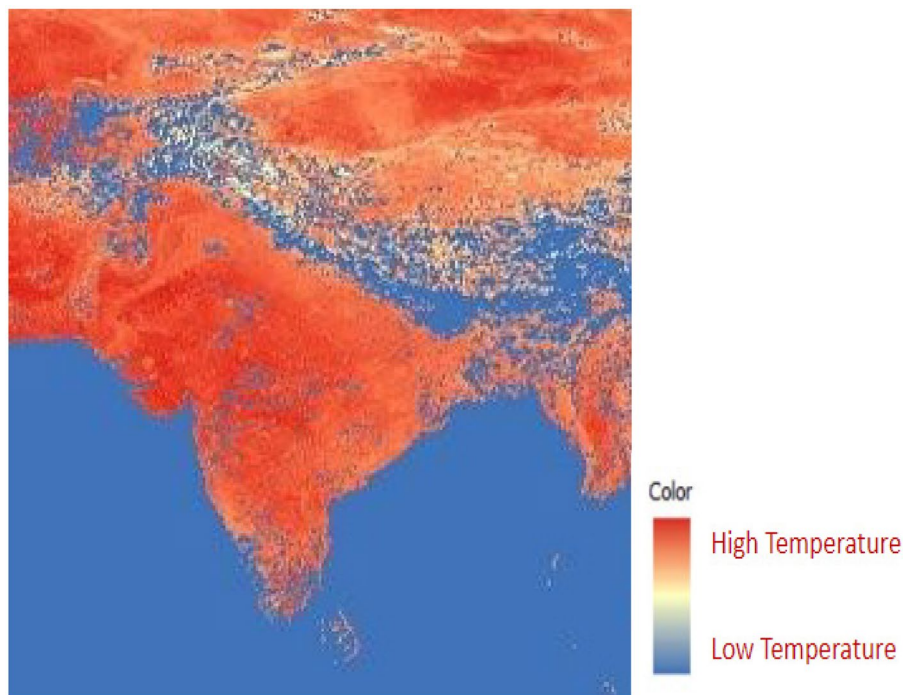
Fig. 6 Land Surface Temperature, Indian Subcontinent, year 2020
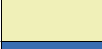
4.2.2 Change in Rainfall Intensity

In most landlocked locations, rainfall replenishes subsurface water and transitory water bodies and contributes to surface water. However, the rainfall pattern and intensity have altered dramatically as a result of fast changes caused by anthropogenic activities.

Thematic maps were created for the research period of 2005–2020 after a brief qualitative study of the PERSIANN's ability to recreate the main rainfall regimes in the Indian subcontinent. Changes in rainfall intensity were estimated using the PERSIANN's data as shown in Fig. 8. Then, the monthly data was averaged to get a normalized result for the two study years. The shape file of India shown in Section 3, Fig. 1 was used to generate the output map.

Regional and interannual rainfall variability is driven by the high uncertainty of ocean-continent surface coupling. In contrast, local spatial–temporal variability is influenced by the structure's great heterogeneity and convection intensity associated with evapotranspiration.

Table 3 Colour Palette Symbology

S. No.	Colour	Hex Code	Pixel Value	Temperature Range(K)
1		#D72F27	16773-14862	335.46 - 297.24
2		#FEFFBD	14862-12887	297.24 - 277.74
3		#4675B5	12887 – 0	277.74–0
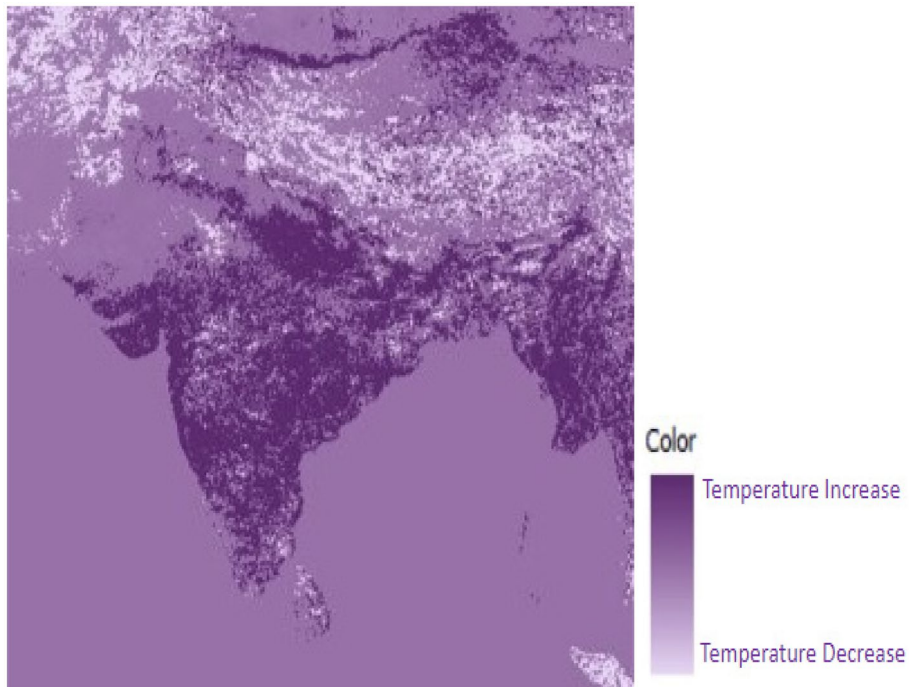
Fig. 7 Difference between Land Surface Temperatures from 2005 to 2020

The increase in rainfall intensity in the peninsula region could be attributed to the recent cyclone Tauktae in the western peninsula during mid-May 2020 and the early onset of monsoon in June 2020.

Table 5 explains the colour symbology and the change trends in rainfall intensity with dark blue showing a significant increase in the rainfall intensity and yellow and red depicting an overall decrease for a range of values as explained in the table.

4.3 Mapping the Relation Between the Surface Water and Causes

In the research, the authors analyzed and established a relation between the various discussed causes and factors with the levels of surface water change, i.e., increase, decrease or no change. All the changes were mapped and plotted for visualization, and pixel by pixel

Table 4 Colour Palette Symbology

S. No.	Colour	Hex Code	Pixel Value	Temperature Difference (K)
1		#5C2C70	17151 - 14152	343.15 – 283.15
2		#9A75A8	14152 - 13652	283.15–273.15
3		#E5D5F3	13652 - 0	273.15 – 223.15
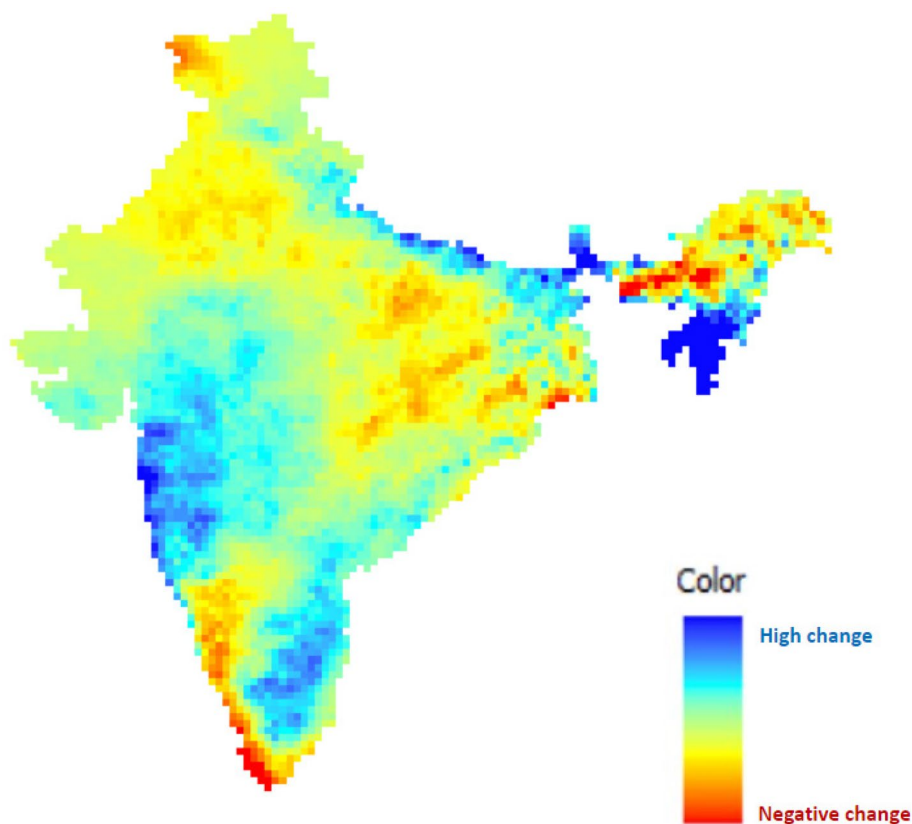
**Fig. 8** Difference in Rainfall intensity from 2005 to 2020

raster calculation was performed to map the changes. A surprising observation was observed that the colour mapping was similar for a few regions such as the western peninsula of India, the Himalayan region and some parts of the east near Bangladesh, as shown in Fig. 9.

Data was extracted for each of these areas and compared to understand the relation between the given parameters. The increase in rainfall and decrease in land surface temperature saw an increase in net overall surface water levels. Similarly, a decrease in rainfall or an increase in land surface temperature corresponded to a decrease in surface water levels. The authors also mapped various water bodies in the study region as shown in Fig. 10. 13 water bodies, namely Ganges, Savitri River, Hooghly River, Krishna River, Brahmaputra

Table 5 Colour Palette Symbology

S. No.	Colour	Hex Code	Rainfall Change (mm)
1		#0001FE	340.17 - 42.0996
2		#02FEFF	42.0996 – 0
3		#FFFF00	0 - (-28.963)
4		#F00100	(-28.963) - (-194.9)
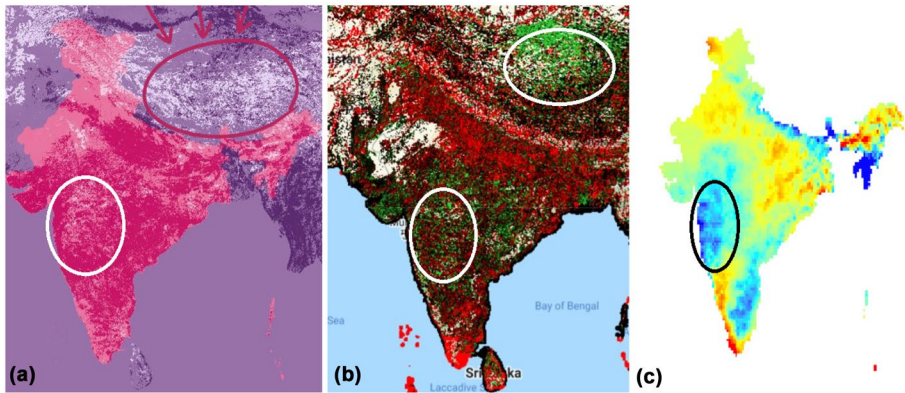
Fig. 9 Comparative analysis of different factors **a** Land Surface Temperature **b** Surface water **c** Rainfall intensity

River, Mahanadi River, Kaveri River, Kollidam River, Godavari River, Netravathi River, Narmada River, Konya River, Dwarakeswar River, Dal Lake were chosen for analysis. The data of these 13 rivers were extracted, and analysis was performed. These water bodies were further used to verify the findings and establish a relation between the various factors discussed in the results Section 5.

5 Results

The variation of surface water in India has various reasons, and the rationale behind this disparity needs to be further scrutinized. Hence, the authors manifested the ramifications of changes in land surface temperature and rainfall intensity on surface water levels. Global warming is known to be one of the biggest reasons for the escalation, like the melting of mountain ice caps in the Himalayas, resulting in a substantial increase in the water levels. Incessant floods in the region during the rainy season and Tauktae, the cyclone which hit the western peninsula during mid-May 2020 result in a significant increase in the surface water. A decrease in surface water levels in other areas was observed where land surface temperature increased significantly.

Following the discussion in Section 4.3, after generating the per-pixel raster maps for the changes in the various environmental factors, 13 Indian water bodies were selected at random on the map and analyzed closely to find a correlation between the various discussed factors. The green points on the raster image of Fig. 11 signify the water bodies that were chosen and analyzed. These rivers were plotted on both the rainfall intensity variation map Fig. 11a and land surface temperature Fig. 11b.

The values were extracted for each of the following rivers. The extracted parameters included latitude, longitude, change in surface water level, change in rainfall intensity in mm, and change in the land surface temperature in Kelvin. Due to large variance in the data, each of these parameters was normalized $x_{normalised}$ using the Formula (2).:

$$x_{normalised} = \frac{x - x_{mean}}{s} \tag{2}$$

Fig. 11 **a** Green dots signify 13 water bodies on the rainfall intensity map. **b** Green dots signify 13 water ▶
bodies on the change in the land surface temperature map

here x is the data value for each river, x_{mean} is the mean of the column or parameter and s
is the standard deviation of each of the discussed parameters. The authors also classified
the rivers into red and green zones i.e., the zone with decrease and increase in the surface
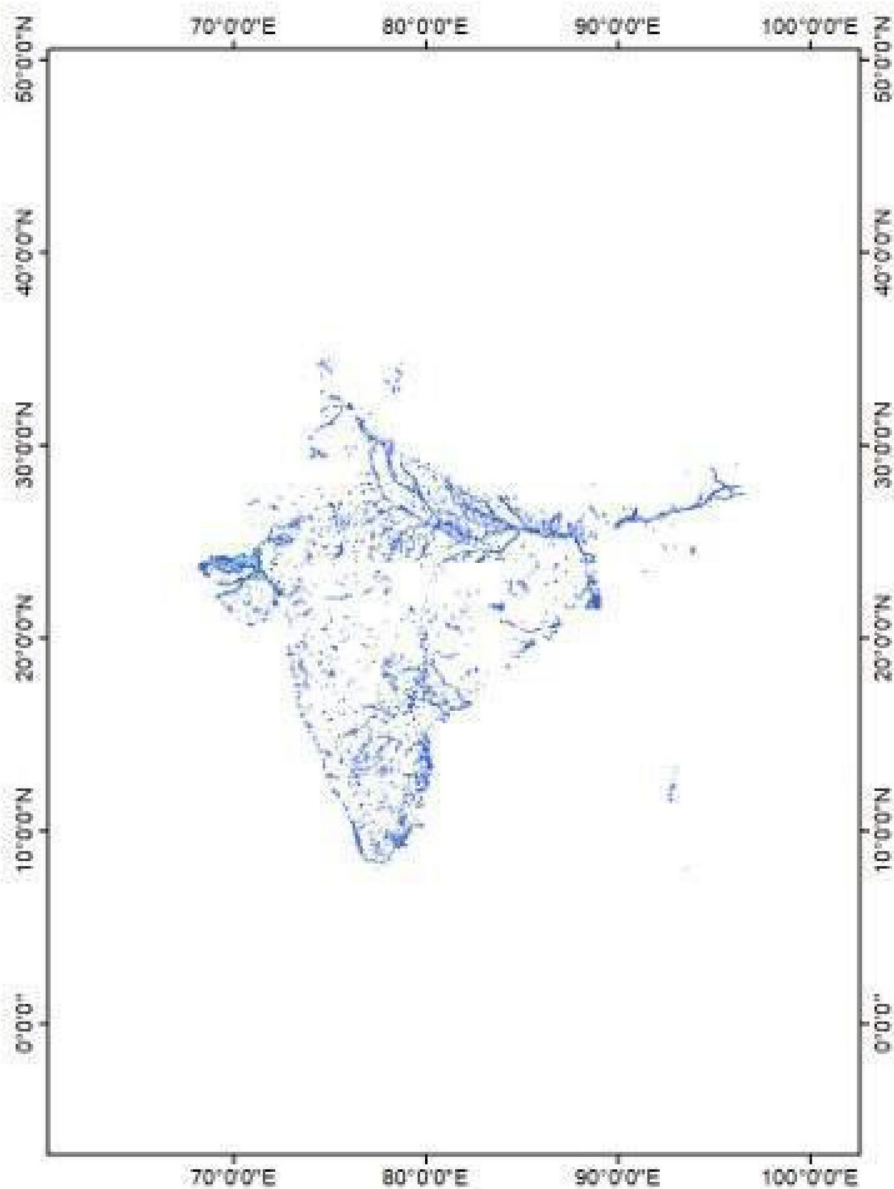
Fig. 10 Water bodies and streams detected in India

(a)
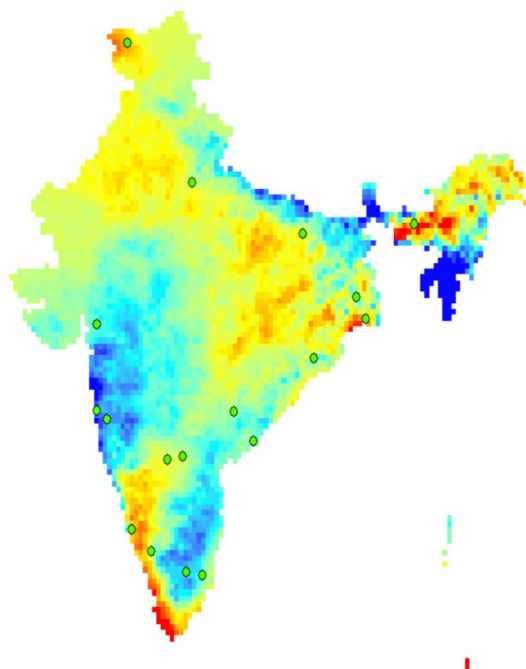
(b)
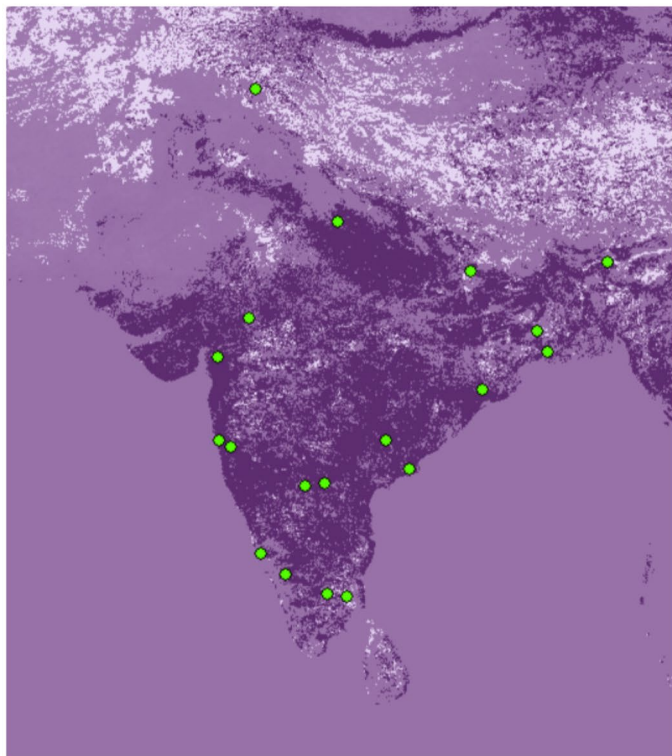
Fig. 12 Rivers with increased surface water from 2005 to 2020

water, respectively as explained in Section 4. Finally, the observations were plotted for all the 13 rivers in Figs. 12 and 13, which were divided on the basis of increase and decrease in the surface water.

The results, as discussed, are divided into two main categories for better identification of features and clearer visualization of results. The graph in Figs. 12 and 13 shows an inverse relationship between the Occurrence change of Surface Water and the Land Surface Temperature, which is also affected by the change in rainfall intensity.

Figure 12 shows the graph for the regions where the surface water levels have increased. The vertical axis shows the normalized value for each of the discussed rivers. Godavari River originates from the north western region of India from the state of Maharashtra and is close to the Arabian Sea. A decrease of -0.42 is observed in the land surface temperature along with an increase in surface water of around 0.46 with a slight decrease in rainfall intensity of nearly 0. This indicates that the surface water shows a positive trend when the temperature of the region is maintained or reduced over the years. Similar patterns were seen for Narmada and Koyna River.
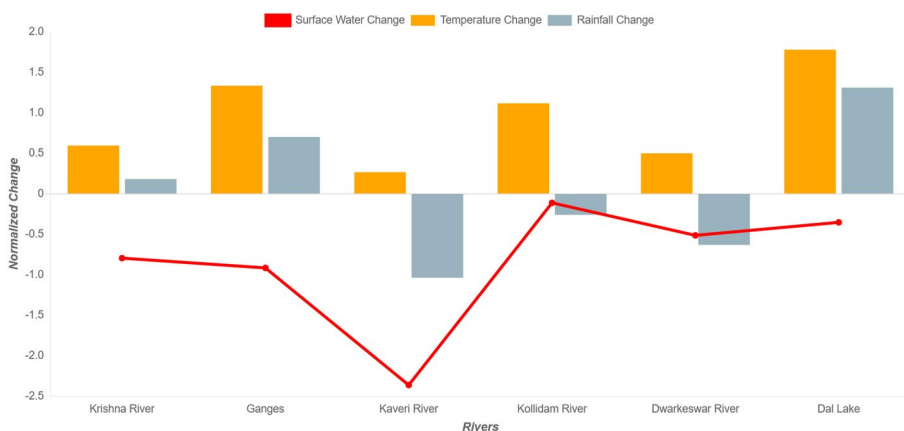
Fig. 13 Rivers with decreased surface water from 2005 to 2020

Narmada River is the fifth largest river in India and originates from Madhya Pradesh. Here, a decrease of –0.9 in Land Surface Temperature is observed and supporting the results, an increase in surface water of 1.31 is observed. The next river in the study was the Kona River. It is a tributary of the Krishna River. This tributary shows an increase in surface water levels in the western Maharashtra region. A decrease in the temperature of –1.02 is also seen when the temperatures of June 2005 and June 2020 were monitored using MODIS Dataset. Along with this, a sharp decrease in the rainfall intensity of over –1.38 can also be seen. Mahanadi River, Netravathi and Kabini River also show the same results as the above and an indirect proportion was observed between the land surface temperature and the surface water level. However, the Brahmaputra River shows a sharp increase in surface water levels even though the land surface temperature shows a small decrease. This was a different case from the rest of the rivers and was considered special. One possibility of this increase is the region's heavy rainfall and melting of glaciers. As the Brahmaputra originates from the Kailash Ranges of the Himalayas, the temperature of the origin point in Tibet of the river was observed and showed an increase over the years. This temperature increase leads to the melting of the glaciers of the Kailash Ranges and hence could be the reason for the abnormal increase in the surface water levels.

Figure 13 shows the rivers where the decrease in Surface water was observed and the temperature and rainfall change intensity. Kaveri River shows an increase in land surface temperature of 4.2 and a decrease in rainfall, which results in an overall decrease in the surface water levels. Kollidam river in the south-eastern region of India and the Dwarakeswar river, a major river in West Bengal, saw a decrease in the net surface water in the 20-year period. The discussed rivers saw an increased land surface temperature by 1.18, 0.56 respectively and a decrease in the rainfall intensity of -0.14 and –0.51, respectively. This observation aligns with the inverse relationship observed. The example of Dal Lake, from Fig. 13 explains that an excessive increase in land surface temperature and a considerable increase in the rainfall accounted for nearly no change in the surface water level. Dal Lake is found in northern India, and increased land surface temperature also results in excessive melting of snow, resulting in increased surface water level. The Ganges, the largest river in India and the Krishna River found in Maharashtra observed a similar trend to Dal Lake. Despite the increase in rainfall, the increase in land surface temperature was comparably high, resulting in a net decrease in surface water.

The authors also observed that the rivers in Fig. 12 correspond to the green-coloured areas (increased surface water) of Fig. 4 in Section. 4.2 and the rivers in Fig. 13 have their latitudes and longitudes in the red coloured region of the same Fig. This shows that the increase in land surface temperature and rainfall are influential factors in the change in surface water levels of India.

Further, a correlation was established between surface water and land surface temperature and rainfall intensity parameters. The correlation coefficient between the two parameters is a scale-free measure of a linear relationship. Table 6 depicts the correlation of surface water with land surface temperature and rainfall intensity change.

Table 6 Correlation of Surface water with Land Surface Temperature and Rainfall Change

Surface Water Change	Impact of Land Surface Temperature	Impact of Change in Rainfall Intensity
Increase in Surface Water	0.19	0.71
Decrease in Surface Water	0.48	0.388

Surface Water Change	R^2_{adj}
Increase in Surface Water	0.41
Decrease in Surface Water	0.359

An increase in the surface water is major because of rainfall change which correlates as 0.71 compared to the 0.19 of land surface temperature, but the decrease in the surface water is because of an increase in land surface temperature correlating to 0.48 and 0.388 correlation of rainfall intensity change. These correlation values were used to find the adjusted R-squared value. To find the same, the authors calculated the R-squared value R^2 which is calculated by the Formula (3).

$$R^2 = \frac{\left(r_{\dot{x}z}\right)^2 + \left(r_{yz}\right)^2 - 2r_{\dot{x}z}r_{yz}r_{xy}}{1 - r_{xy}^2} \tag{3}$$

The variable x corresponds to a change in Land surface temperature, and y corresponds to a change in rainfall intensity which is independent variables here. Variable z in the change in surface water which is the dependent variable. This gives the multiple correlation coefficient. R^2_{adj} is used to calculate the adjusted R-squared value using the Formula (4).

$$R^2_{adj} = 1 - \frac{\left(1 - R^2\right)(n - 1)}{n - k - 1} \tag{4}$$

Here k is the number of independent variables, which is 2 in this case, and n is the number of data elements. Table 7 gives the R^2_{adj} value which explains a 41% dependence of increase in surface water on land surface temperature and rainfall and the value of 35.9% dependence of decrease in surface water on land surface temperature and rainfall. Both the values are nearly equal, which corresponds to the observations. The average R^2_{adj} value is 0.402.

6 Conclusion

6.1 The Research Issue and Major Findings

The authors discussed the relationship between the surface water change and with change in land surface temperature and rainfall intensity. Google Earth Engine Code Editor with Python API was used to detect changes in the trends of surface water levels and quantify differences in the map trends between the years 2005 and 2020. ArcMap was used to make raster calculations on the datasets obtained. The study on 13 water bodies across India established that the changes in Surface Water Levels to be the causation of Global Warming, which also results in unpredictable precipitation. The purpose of the research was to relate the change in the land surface temperature and rainfall levels using the geo-stationary satellite data to determine the cause of the decline in the surface waters of India. However, an increase in surface water in certain regions was also observed, which can also be attributed to global warming and the excessive rainfall in western peninsula or melting ice caps in the Himalayan region, leading to flooding of riverbanks and disrupting human activities like agriculture.

The authors also calculated an average R-squared value of 0.402 between the dependent variable (change in surface water) and multi-independent variables (change in land surface temperature and change in rainfall intensity), which will be helpful in mapping other causes for the change in levels of surface water. This work opens up the possibility of finding more issues in relation to the alteration in surface water levels caused by global warming.

The machine learning and data analysis approach developed in this study has useful and greater applicability in other regions of the world.

6.2 Areas for Further Research

Progress has been made in the field of remote sensing to monitor various environmental trends over the years to better understand the current state of the globe as well as to predict the upcoming events in order to prevent catastrophic results, but many important research questions still remain unanswered. This research is an initiative that gives priority to perform more research on surface water trends and should be continued to improve the current condition. Further machine learning models can be developed using the previous trends of surface water change with attributes like soil erosion, humidity, temperature and rainfall trends to predict the change in the levels in the coming years and determine the most impactful attributes among these.

References

Al Kafy A, Al Rakib A, Akter KS, Rahaman ZA, Jahir DM, Subramanyam G, Bhatt A (2021) The operational role of remote sensing in assessing and predicting land use/land cover and seasonal land surface temperature using machine learning algorithms in Rajshahi, Bangladesh. Appl Geomat 1–24

Alsdorf DE, Rodríguez E, Lettenmaier DP (2007) Measuring surface water from space. Rev Geophys 45(2)

Barakat A, Ouargaf Z, Khellouk R, El Jazouli A, Touhami F (2019) Land use/land cover change and environmental impact assessment in béni-mellal district (Morocco) using remote sensing and gis. Earth Syst Environ 3(1):113–125

Downing JA, Prairie YT, Cole JJ, Duarte CM, Tranvik LJ, Striegl RG, Middelburg JJ (2006) The global abundance and size distribution of lakes, ponds, and impoundments. Limnol Oceanogr 51(5):2388–2397

Ghorbani K, Salarijazi M, Ghahreman N (2022) Development of stepwise m5 tree model to determine the influential factors on rainfall prediction and overcome the greedy problem of its algorithm. https://doi.org/10.21203/rs.3.rs-1260445/v1. PPR:PPR449276

Huang C, Chen Y, Zhang S, Wu J (2018) Detecting, extracting, and monitoring surface water from space using optical sensors: A review. Rev Geophys 56(2):333–360

India-WRIS wiki (2015) https://www.indiawris.gov.in/wris/#/

Jiang H, Feng M, Zhu Y, Lu N, Huang J, Xiao T (2014) An automated method for extracting rivers and lakes from Landsat imagery. Remote Sens 6(6):5067–5089

JRC Global Surface Water (2000) https://developers.google.com/earth-engine/

Mehrazar A, Bavani ARM, Gohari A, Mashal M, Rahimikhoob H (2020) Adaptation of water resources system to water scarcity and climate change in the suburb area of megacities. Water Resour Manag 34(12):3855–3877

MODIS Land Surface Temperature (2000) https://modis.gsfc.nasa.gov/data/dataprod/

Mustafa EK, Co Y, Liu G, Kaloop MR, Beshr AA, Zarzoura F, Sadek M (2020) Study for predicting land surface temperature (LST) using landsat data: a comparison of four algorithms. Adv Civil Eng

Nguyen P, Shearer EJ, Tran H, Ombadi M, Hayatbini N, Palacios T, Sorooshian S (2019) The CHRS Data Portal, an easily accessible public repository for PERSIANN global satellite precipitation data. Sci Data 6(1):1–10

Pekel JF, Cottam A, Gorelick N, Belward AS (2016) High-resolution mapping of global surface water and its long-term changes. Nature 540(7633):418–422

Pérez-Alarcón A, Garcia-Cortes D, Fernández-Alvarez JC, Martínez-González Y (2022) Improving monthly rainfall forecast in a watershed by combining neural networks and autoregressive models. Environ Process 9(3):1–26

PERSIANN Precipitation Data (2000) https://chrsdata.eng.uci.edu/

Prigent C, Papa F, Aires F, Rossow WB, Matthews E (2007) Global inundation dynamics inferred from multiple satellite observations, 1993–2000. J Geophys Res Atmos 112(D12)

Prigent C, Papa F, Aires F, Jimenez C, Rossow WB, Matthews E (2012) Changes in land surface water dynamics since the 1990s and relation to population pressure. Geophys Res Lett 39(8)

Puppala H, Singh AP (2021) Analysis of urban heat island effect in Visakhapatnam, India, using multi-temporal satellite imagery: causes and possible remedies. Environ Dev Sustain 23(8):11475–11493

Shakeel A, Sultani W, Ali M (2019) Deep built-structure counting in satellite imagery using attention based re-weighting. ISPRS J Photogramm Remote Sens 151:313–321

Shindell DT, Faluvegi G, Bell N, Schmidt GA (2005) An emissions-based view of climate forcing by methane and tropospheric ozone. Geophys Res Lett 32(4)

Singh AP, Dhadse K (2021) Economic evaluation of crop production in the Ganges region under climate change: A sustainable policy framework. J Clean Prod 278:123413

Tang Y, Xi S, Chen X, Lian Y (2016) Quantification of multiple climate change and human activity impact factors on flood regimes in the Pearl River Delta of China. Adv Meteorol

Taylor RG, Scanlon B, Döll P, Rodell M, Van Beek R, Wada Y, Treidel H (2013) Ground water and climate change. Nat Clim Change 3(4):322–329

Vorosmarty CJ, Green P, Salisbury J, Lammers RB (2000) Global water resources: vulnerability from climate change and population growth. Science 289(5477):284–288

Wan Z (2008) New refinements and validation of the MODIS Land-Surface Temperature/Emissivity products. Remote Sens Environ 112(1):59–74. https://doi.org/10.1016/j.rse.2006.06.026

Wolfe RE (2006) MODIS geolocation. In Earth science satellite remote sensing (pp. 50-73). Springer, Berlin, Heidelberg

Xia J, Zeng J (2022) Environmental factors assisted the evaluation of entropy water quality indices with efficient machine learning technique. Water Resour Manag 36(6):2045–2060

Zha Y, Gao J, Ni S (2003) Use of normalized difference built-up index in automatically mapping urban areas from TM imagery. Int J Remote Sens 24(3):583–594

Zhang X, Ma L, Zhu Y, Lou W, Xie B, Sheng L, Gu Q (2022) Temporal stability analysis for the evaluation of spatial and temporal patterns of surface water quality. Water Resour Manag 36(4):1413–1429

Authors and Affiliations

Vanita Jain[1] · Aarushi Dhingra[1] · Eeshita Gupta[1] · Ish Takkar[1] · Rachna Jain[2] · Sardar M. N. Islam[3] ID

Vanita Jain
vanita.jain@bharatividyapeeth.edu

Aarushi Dhingra
aarushidhingra99@gmail.com

Eeshita Gupta
eeshita.gupta1909@gmail.com

Ish Takkar
ishtakkar21@gmail.com

Rachna Jain
rachnajain@bpitindia.com

[1]   Bharati Vidyapeeth's College Of Engineering, New Delhi, India

[2]   Bhagwan Parshuram Institute of Technology, New Delhi, India

[3]   ISILC, Victoria University, Footscray, Australia